



Effect of particle size on the convective heat transfer in nanofluid in the developing region

K.B. Anoop, T. Sundararajan, Sarit K. Das *

Heat Transfer and Thermal Power Laboratory, Department of Mechanical Engineering, Indian Institute of Technology – Madras, Chennai 600 036, India

ARTICLE INFO

Article history:

Received 25 June 2007

Received in revised form 5 October 2007

Available online 3 February 2009

Keywords:

Nanofluid

Particle size effect

Forced convection

Nano-suspensions

Entrance length

ABSTRACT

An experimental investigation on the convective heat transfer characteristics in the developing region of tube flow with constant heat flux is carried out with alumina–water nanofluids. The primary objective is to evaluate the effect of particle size on convective heat transfer in laminar developing region. Two particle sizes were used, one with average particle size of 45 nm and the other with 150 nm. It was observed that both nanofluids showed higher heat transfer characteristics than the base fluid and the nanofluid with 45 nm particles showed higher heat transfer coefficient than that with 150 nm particles. It was also observed that in the developing region, the heat transfer coefficients show higher enhancement than in the developed region. Based on the experimental results a correlation for heat transfer in the developing region has been proposed for the present range of nanofluids.

© 2009 Elsevier Ltd. All rights reserved.

1. Introduction

Improving the heat transfer characteristics of a coolant liquid had been in research for decades. The slurries used for this purpose have inherent problem of sedimentation, clogging of channels and higher pressure drops causing significant component erosion as they use micron sized particles. With the advent of material science and sophisticated techniques of producing nano-sized particles, more research work in suspending those nanoparticles in the coolant fluid came into light. The pioneering work of suspending nano-sized particles in a fluid (nanofluids) was carried out by Choi and co-workers [1] at Argonne National Laboratory and showed a considerable increase in thermal conductivity of the liquid. Lee et al. [2] reported that the suspension of 4.0 vol % 35 nm CuO particles in ethylene glycol showed 20% increase in effective thermal conductivity. Das et al. [3] investigated the temperature dependence of thermal conductivity enhancement in nanofluids experimentally. This dependence was established as they observed a 2- to 3-fold increase in thermal conductivity enhancement of nanofluid over a temperature range of 21–51 °C. It was also comprehended that theoretical models such as Maxwell [4] and Hamilton–Crosser [5] under-predicts the thermal conductivity of nanofluids.

Following a series of studies on thermal conductivity, the investigation on convective heat transfer in nanofluids began. However even before the above studies on conduction, Pak and Cho [6] investigated convective heat transfer in the turbulent flow regime

using water–Al₂O₃ and water–TiO₂ nanofluids experimentally, and found that the Nusselt number of the nanofluids increases with increasing volume fraction of the suspended nanoparticles and Reynolds number. Xuan and Li [7] measured convective heat transfer coefficient of water–Cu nanofluids, in turbulent regime and found considerable heat transfer enhancement. Also Xuan and Roetzel [8] were the first to indicate a mechanism for convective heat transfer in nanofluids. They proposed thermal dispersion as a major mechanism of heat transfer in flowing fluid, along with the enhancement of nanofluid thermal conductivity. Laminar heat transfer in the entrance region of a tube flow was the focus of the work by Wen and Ding [9] using alumina–water nanofluid. Viscosity of the nanofluid was assumed to follow the traditional Einstein equation for suspensions. For the nanofluid that contained 1.6% nanoparticles by volume, the local heat transfer coefficient at the entrance region was 41% higher than that with the base fluid at the same flow rate. It was observed that the enhancement is particularly significant in the entrance region and decreases with axial distance. The thermal entry length of nanofluids was greater than that of the pure base liquid and was found to increase with an increase in particle concentration. Particle migration [10] was proposed as a reason for the enhancement, which led to a non-uniform distribution of thermal conductivity and viscosity field and reduced the thermal boundary layer thickness. Convective heat transfer of CNT nanofluids in laminar regime with a constant heat flux wall boundary condition was investigated by the same authors [11]. An observed maximum enhancement of 350% at Re = 800 for 0.5 wt% CNTs clearly reveals that enhancement of the convective heat transfer coefficient was much more dramatic than that purely due to the enhancement of effective thermal conductivity.

* Corresponding author. Tel.: +91 44 2257 4655; fax: +91 44 2257 4652.
E-mail address: skdas@iitm.ac.in (S.K. Das).

Nomenclature

C_p	specific heat [J/kg K]
d	diameter [m]
D	diameter of the tube [m]
k	thermal conductivity [W/m K]
Nu	Nusselt number
Pr	Prandtl number
q''	heat flux [W/m ²]
Re	Reynolds number
T	temperature [K]
x	distance along axis [m]
x_+	$x/(D Re Pr)$

Greeks

η	viscosity [Pa s]
ϕ	volume fraction

Subscripts

bf	base fluid
f	fluid
H	constant heat flux
in	inlet
nf	nanofluid
p	particle
r	relative
w	wall

Enhancement of the experimental convective heat transfer coefficient of graphite nanoparticles dispersed in liquid for laminar flow in a horizontal tube heat exchanger was reported by Yang et al. [12]. The experimental results illustrated that the heat transfer coefficient increases with the Reynolds number and the particle volume fraction and decreases with fluid temperature. Nguyen et al. [13] experimentally probed into the heat transfer enhancement of Al₂O₃–water nanofluid, flowing inside a closed system, destined for cooling of a microprocessor or other electronic components. In the turbulent regime with 6.8% particle volume concentration, heat transfer coefficient was found to be increased by as much as 40% compared to that of the base fluid. Experimental data showed that the nanofluid with 36 nm particle diameter provided higher heat transfer coefficients than the ones with 47 nm particle size. An experimental study was carried out on the flow and heat transfer behaviour of aqueous TiO₂ nanofluids flowing through a straight vertical pipe under both the laminar and turbulent flow conditions by He et al. [14]. Three average particle sizes of 95 nm, 145 nm and 210 nm were obtained by using different processing techniques were used. Given the flow Reynolds number and particle size, the convective heat transfer coefficient increased with nanoparticle concentration in both the laminar and turbulent flow regimes and the effect of particle concentration was more in the turbulent flow regime. For a fixed particle concentration and flow Reynolds number, the convective heat transfer coefficient seemed to be less sensitive to the average particle size under the conditions of this work. The small effect of particle size on the convective heat transfer coefficient could be due to particle migration as well as particle size distribution. Heris et al. [15,16] presented the experimental results of the convective heat transfer of CuO/water and Al₂O₃/water nanofluids inside a circular tube with constant wall temperature. It was emphasized that, the increase in heat transfer coefficient due to the presence of nanoparticles was much higher than the prediction of single-phase heat transfer correlation using nanofluid effective properties. However, the Al₂O₃/water nanofluid showed higher enhancement when compared to CuO/water.

Roy et al. [17] and Palm et al. [18] numerically investigated the forced convective heat transfer of nanofluids. They considered local thermal equilibrium and assumed that the nanofluid behaves as a conventional single-phase fluid with properties evaluated as functions of those of the constituents, knowing their respective concentrations. In another recent study, using a two-component, four-equation, non-homogeneous equilibrium model for convective transport, Boungiorno [19] conducted a numerical study of the turbulent heat transfer of nanofluids. In the model, the wall layer consisted of two regions, the viscous sub-layer and the turbulent

sub-layer. Viscosity and particle volume fraction were less in the viscous sub-layer, whereas conductivity in that region was greater. The heat transfer enhancement was explained mainly by a reduction in viscosity within and consequent thinning of the viscous sub-layer, and a new correlation was developed that agrees with existing experimental results. Thermophoresis was argued to have a major effect in bringing this non-uniform distribution of particles.

Daungthongsuk and Wongwises [20] summarized and reviewed the published articles pertinent to the forced convective heat transfer of nanofluids for both experimental and numerical investigations.

From the above literature review it may be noted that higher enhancements in heat transfer coefficients were observed in the entrance region but studies on the effect of particle sizes in this region has not been investigated comprehensively. Hence, the present study concentrates on the heat transfer enhancement in the laminar developing region with varying particle sizes and concentrations. The nanofluid used in the present study is alumina–water with average particle sizes of 45 nm and 150 nm. The particle concentrations used in the experiments were of 1 wt%, 2 wt%, 4 wt% and 6 wt%.

2. Experiments

The experimental approach mainly consists of preparation of a stable nanofluid, evaluating the thermal and physical properties and conducting convective heat transfer studies using it. These are described in the sections below.

2.1. Nanofluid preparation

Preparation of a stable nanofluid is quite an involved task. Commercially purchased nano-powders (Nanophase Technologies Corporation and Inframat Advanced Materials) produced by Laser evaporated physical methods were used to make the nanofluids. Nanofluids were prepared by top-down approach in which nanoparticles were suspended in the base fluid (here water). Fig. 1 shows the TEM of typical Al₂O₃ particles used. These figures (a) and (b) reconfirm the average size as specified by the manufactures (using nitrogen gas absorption technique) to be in the range 45 nm (Nanophase Technologies Corporation, Al₂O₃, Purity 99.5%, APS 45 nm (determined from SSA), SSA = 45 m²/g (BET), Crystal Phase = 70:30, Delta: Gamma) and 150 nm (Inframat Corporation, purity 99.8%, 100% alfa phase, average particle size 150 nm, (from BET SSA and SEM), BET multi-point specific surface area (SSA) ~10 m²/g), respectively. Fig. 1(c) indicates particle size distribution

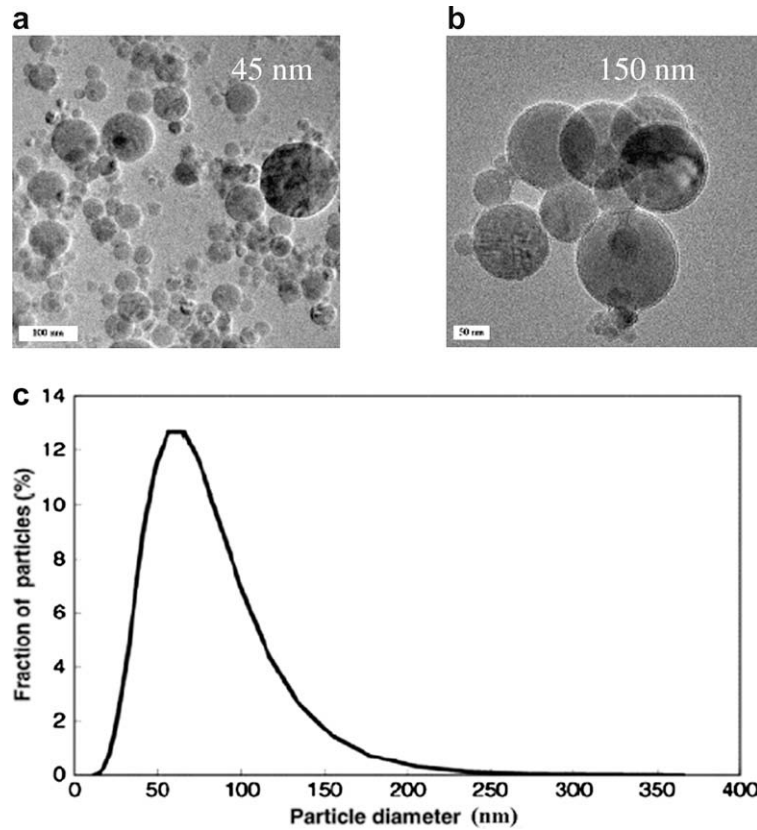


Fig. 1. TEM of nanoparticles used: (a) 45 nm, (b) 150 nm, (c) particle size distribution for nanoparticles with average size 45 nm.

as provided by manufactures for an average particle size of 45 nm. The particles were further dispersed in the suspension using ultrasonication which breaks down the agglomerates formed in air. Further stability is achieved by keeping the pH value away from the iso-electric point (IEP) which is the point with zero zeta potential (and hence maximum attraction between the particles). The pH values used for 1 wt%, 2 wt%, 4 wt% and 6 wt% were 6.5, 6, 5.5 and 5, respectively (IEP of Al₂O₃ is 9.2). A minimum of 2.5 l of each concentrations were prepared and it was observed that the suspensions were stable for several weeks.

2.2. Effective thermal conductivity and viscosity

The thermal conductivities of the suspensions were measured using the standard transient hotwire method. In this method, a thin metallic wire is used as a line heat source as well as thermometer. The wire is surrounded by the liquid whose thermal conductivity is to be measured. The wire is then heated by sending current through it. Now, higher the thermal conductivity of the liquid, lower will be the rate of temperature rise of the wire. This principle is used to measure the thermal conductivity using the expression for heat transfer in a semi-infinite medium with a line heat source. The experiment lasts for a maximum of 4 s hence this is a very fast method which can avoid onset of natural convection [21]. The thermal conductivity values measured were within an uncertainty range of ±2%. The relative viscosities of nanofluid were measured using an Ubbelohde viscometer. It works on the principle of evaluating the time required for a particular quantity of fluid to pass through a capillary bore. The above comparative viscometer had a capillary bore of 0.5 mm. The ratio of efflux time of nanofluid, t_{nf} to that of base-fluid t_{bf} was regarded as the experimental relative viscosity ratio.

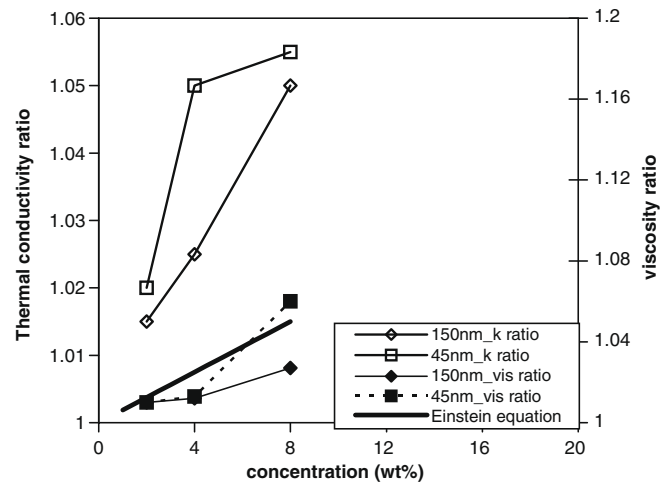


Fig. 2. Variation of thermal conductivity ratio and viscosity ratio with concentration at 30 °C.

$$\text{i.e., } \eta_r = \frac{t_{nf}}{t_{bf}} \tag{1}$$

The time was measured with an accuracy of 0.5 s and the total experimental time involved was 50–100 s; thus the inaccuracy involved in the determination of viscosity ratio was approximately 0.5–1%.

Fig. 2 shows the variation of thermal conductivity ratios and viscosity ratios for different concentrations and two particle sizes. It may be noticed here that as particle size reduces the thermal conductivity of the nanofluid gets increased. Also the thermal

conductivity and viscosity value increase with particle concentration. Thermal conductivity variations at different temperatures of the nanofluids were also measured and the corresponding values were used for the evaluation of Nu in the convective heat transfer analysis due to well known temperature effect on nanofluid conductivity. Regarding viscosity, Einstein's theory seems to predict the viscosities for 150 nm and 45 nm nanofluids more or less correctly. Thus Einstein's equation,

$$\eta_{nf} = \eta_{bf}(1 + 2.5\phi) \quad (2)$$

which is valid for dilute suspensions of spherical particles may be used with confidence for nanofluids with larger particle sizes.

2.3. Convective experimental setup

The work primarily tries to investigate the convective heat transfer behaviours of water based alumina nanofluids with two average particle dimensions. The convective heat transfer mainly in the entrance region of the flow is considered. Fig. 3 shows the schematic diagram of the convective loop used for the investigation. The loop consists of a pump, a heated test section, a cooling section and a collecting tank. The laminar flow in the loop was maintained with the help of a pump whose power supply was controlled by a servo stabilizer which helps in maintaining a constant flow rate during a particular experiment. The flow rates were varied during a set of experiments with the help of a dimmerstat connected to the pump. The heater section was made of copper tube of 1200 mm length and 4.75 ± 0.05 mm inner diameter. The thickness of the tube was around 1.25 mm. Electrically insulated nickel-chrome wire was uniformly wound along the length giving a maximum power of 200 W. A DC power supply was used as a power source to the heater. Calibrated seven T-type thermocouples were brazed on the surface of the copper tube which measured the surface temperatures along the length of the tube. They were positioned along the length at $x/D = 10, 21, 63, 105, 147, 200$ and 244, where x is the distance along the length from the entrance. The inlet and outlet temperatures were measured by two T-type thermocouples immersed in the mixing chambers provided at inlet and exit. Care was taken to maintain plug flow at the entrance using a series of wire meshes. The fluid after passing through the heater section flows through a cooling unit which is a heat exchanger and is collected in a collecting tank. The flow rates were measured by collecting the fluid for a period of time with the help of a precise measuring jar and stop watch.

2.4. Data reduction

Analysis of the heat transfer behaviour of the nanofluids is made by the evaluation of the local heat transfer coefficient and local Nusselt number which are defined as

$$Nu(x) = \frac{h(x)D}{k} \quad (3)$$

$$h(x) = \frac{q''}{(T_w(x) - T_f(x))} \quad (4)$$

where q'' is the heat flux, D is diameter of the tube, and k the thermal conductivity of the fluid and T_w and T_f are the local wall and fluid temperatures and T_f is evaluated from the heat balance as given below. It was observed that the energy balance ratio, which is the ratio of power input to the heater tube to the heat taken away by the fluid, was always above 0.96 and hence,

$$T_f = T_{in} + \frac{q''PDx}{\dot{m}C_p} \quad (5)$$

The thermal conductivity value used was at the bulk mean temperature. The density and specific heat of the nanofluid was evaluated using averaged volume fraction ratio which is generally acceptable.

$$\rho_{nf} = (1 - \phi)\rho_{bf} + \phi\rho_p \quad (6)$$

$$(\rho C_p)_{nf} = (1 - \phi)(\rho C_p)_{bf} + \phi(\rho C_p)_p \quad (7)$$

All the non-dimensional quantities were evaluated based on the properties measured or derived as above. The Prandtl number was defined as $Pr = \nu/\alpha$, where ν is the kinematic viscosity and α is the thermal diffusivity ($k/\rho C_p$). The temperatures were measured with an accuracy of 0.15°C . The uncertainty in the measurement of thermal conductivity was less than 2% and that for viscosity was 0.5%. The systematic uncertainty analysis was carried out for derived quantities and the maximum error in the Re and Nu values were evaluated to be around 3.24% and 2.45%, respectively.

3. Results and discussion

Initially experiments are conducted with water which forms the basis for comparison of results with nanofluids as well as validation of the experimental apparatus. Fig. 4 shows the variation in Nusselt number along the non-dimensional length of the tube. The comparison of the experimental data with the existing correla-

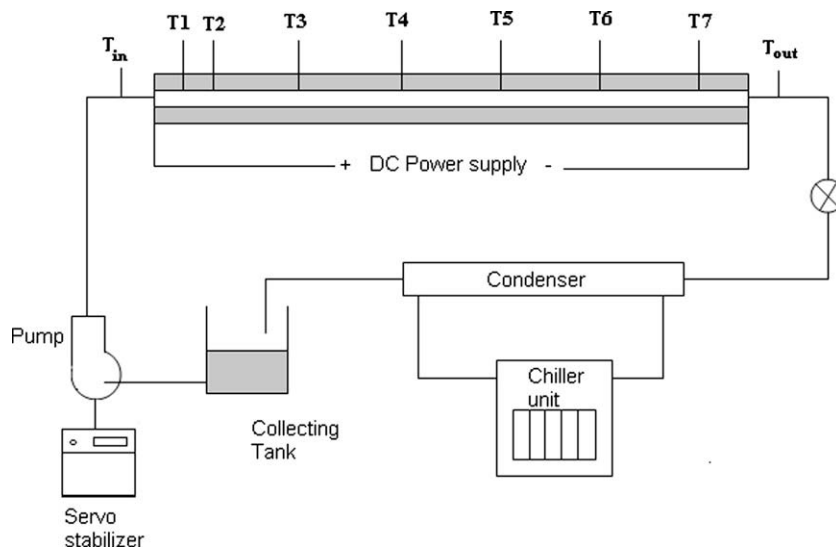


Fig. 3. Schematic of the experimental setup.

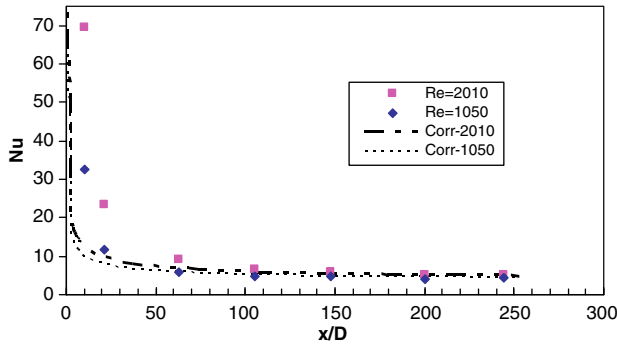


Fig. 4. Validation of the experimental setup.

tion for developing flow [22] shows reasonable agreement except for positions, $x/D = 10$ and $x/D = 21$. Results for two flow rates are shown here. The correlation plotted in the figure is for a simultaneously developing flow for a constant heat flux condition and is given as

$$\begin{aligned}
 Nu_{x,H} &= 3.302x_+^{-1/3} - 1 \quad \text{for } x_+ \leq 0.0005 \\
 &= 1.302x_+^{-1/3} - 0.5 \quad 0.0005 \leq x_+ \leq 0.0015 \\
 &= 4.364 + 8.68(10^3x_+)^{-0.506} e^{-41x_+} \quad x_+ \geq 0.0015
 \end{aligned} \tag{8}$$

where $x_+ = \frac{x}{D} \frac{\rho \mu}{\text{Re Pr}}$ and subscript H stands for a constant heat flux case.

Thus it may be inferred that beyond $x/D = 50$ the deviation from the correlation is within the acceptable limit and the results may be accepted with confidence. The edge heat losses may be the reason for inaccuracy in the region $x/D < 50$. For the nanofluids only experimental data for $x/D > 50$ is considered for this reason. After having carried out sufficient experiments with the base fluid and removing some systematic errors, experiments were conducted with nanofluids.

Fig. 5 shows variation of heat transfer coefficient with different Re at an axial location, $x/D = 147$ for nanofluid with 150 nm particle size at various particle concentrations. This shows the effect of particle concentration. It is evident that nanofluids give higher heat transfer coefficients compared to the base fluid. With the increase in concentration the heat transfer coefficient gets increased. A similar plot for 45 nm based nanofluid is shown in Fig. 6. The figure shows that although the trend is similar to larger particle size, the magnitude of enhancement is greater with smaller particles. Fig. 7 shows the variation of heat transfer coefficient along the length of the tube for 4 wt% concentration for the two particle

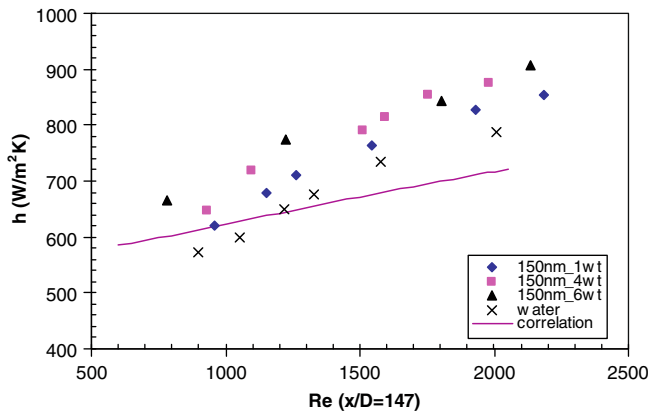


Fig. 5. Heat transfer coefficient variation with Re at $x/D = 147$ for 150 nm based nanofluid.

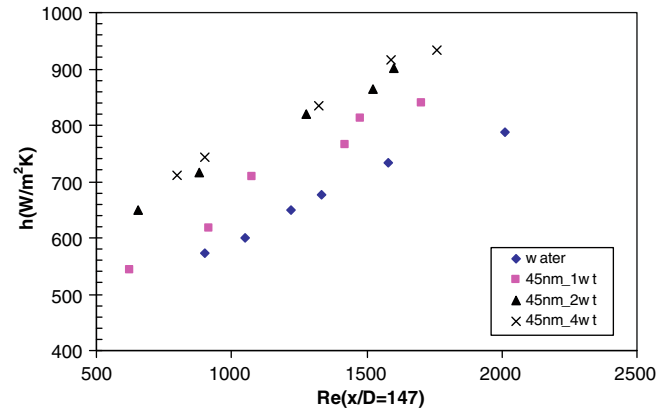


Fig. 6. Heat transfer coefficient variation with Re at $x/D = 147$ for 45 nm based nanofluid.

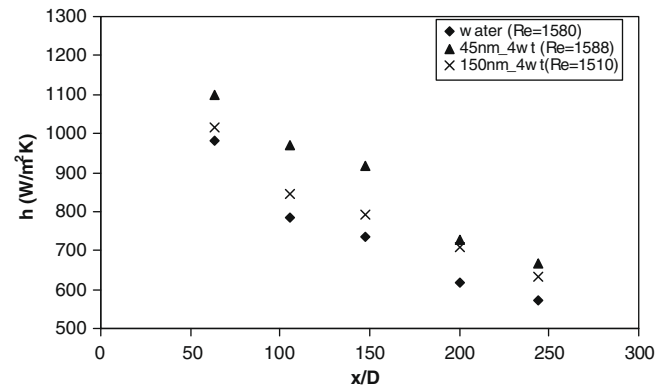


Fig. 7. Effect of particle size on heat transfer coefficient at $Re \sim 1550$.

sizes. The Re is of the order of 1550 and the values beyond $x/D = 50$ are only considered. It may be observed here that as particle size reduces the heat transfer coefficient increases. Also the increase is more predominant in the entrance region, i.e., at lower x/D . Nanofluids with 45 nm particle size gave more enhancement in heat transfer coefficient than that of 150 nm based nanofluid as well as water. In order to conclude whether the increase in heat transfer coefficient is brought about by increase in thermal conductivity or other thermophysical properties, a dimensional and a non-dimensional plot of heat transfer coefficient is made and compared. Fig. 8(a) shows the dimensional heat transfer variation for 150 nm and 45 nm based nanofluids at 4 wt% with varying Re, whereas Fig. 8(b) shows the non-dimensional heat transfer variation for the same case. Here the Nu is calculated based on the thermal conductivity values measured at that concentration, particle size and average bulk fluid temperature. From this plot it may be inferred that the increase in the heat transfer coefficient is much higher compared to the increase in thermal conductivity enhancement. At $x/D = 147$, for 45 nm based nanofluid at $Re = 1550$, the enhancement in heat transfer coefficient is around 25% whereas the thermal conductivity for the same has increased only by 6%. Similarly for 150 nm based nanofluids the heat transfer coefficient enhancement is around 11%, whereas the thermal conductivity increase was around 4% only. Thus, it may be observed that in convective heat transfer with nanofluids some effects beyond the increase in thermal conductivity is occurring which may be due to particle migration effects [10] and/or thermal dispersion [8]. To visualize the effect of developing region a plot of heat transfer coefficient variation with Re at different x/D is made for 45 nm

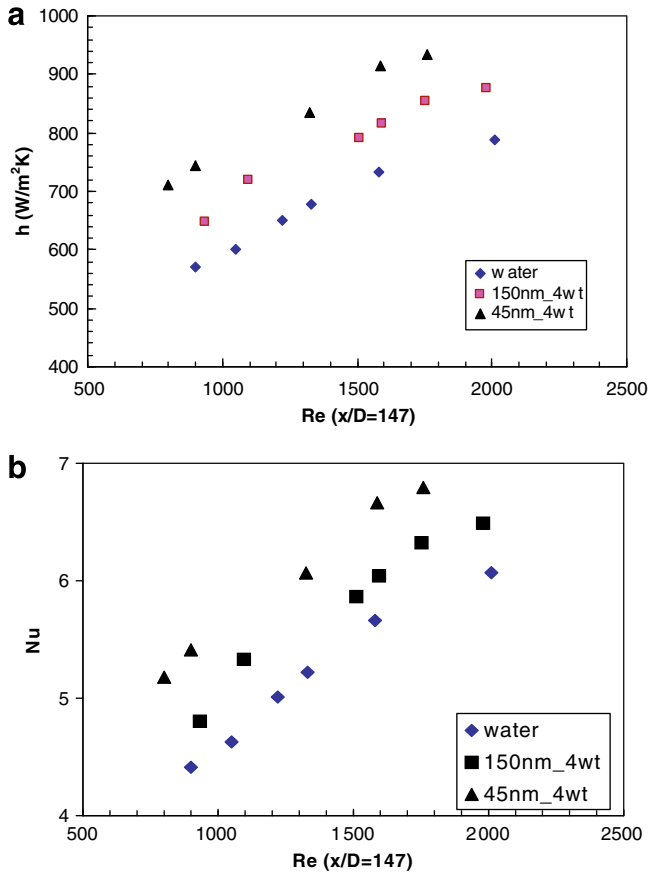


Fig. 8. (a) Dimensional variation of heat transfer coefficient. (b) Non-dimensional variation of heat transfer coefficient.

based nanofluids and for water as shown in Fig. 9. It can be observed that at lower x/D the heat transfer coefficient varies with Re and at $x/D > 200$ it becomes independent of Re . It may be also observed that the enhancement is also more at the entrance region than at a higher x/D . For instance at $Re \sim 1550$, the enhancement in heat transfer coefficient is 31% at $x/D = 63$, whereas it is 25% and 10% at $x/D = 147$ and 244, respectively. Thus it is better to apply nanofluids in the developing region as more particle migration and/or other unknown effects exists, leading to higher thermal dispersion, thus giving higher performance.

After conducting sufficient number experiments with nanofluids, a correlation is tried to be proposed. The correlation which is valid for alumina nanofluids in the developing region $50 < x/D < 200$ for laminar flow with $500 < Re < 2000$ is derived using non-linear regression analysis and is presented below.

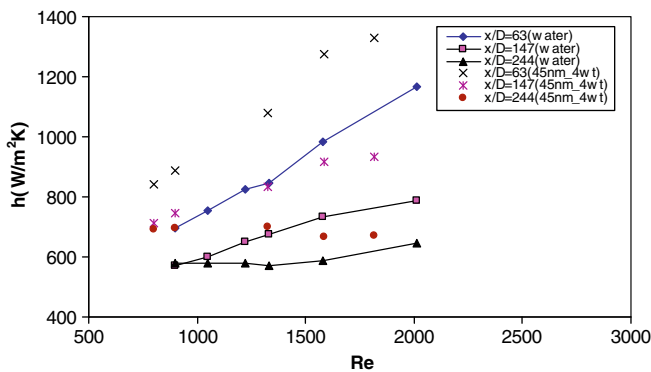


Fig. 9. Effect of axial position on heat transfer of nanofluid.

$$Nu_x = 4.36 + [a.x_+^{-b}(1 + \phi^c).exp(-d.x_+)] \left[1 + e.\left(\frac{d_p}{d_{ref}}\right)^{-f} \right] \quad (9)$$

where $a = 6.219 \times 10^{-3}$, $b = 1.1522$, $c = 0.1533$, $d = 2.5228$, $e = 0.57825$, $f = 0.2183$, $d_{ref} = 100$ nm, $d_p = diameter$ of particle in nm, $\phi = volume$ fraction in percentage.

A parity plot for the above correlation is shown in Fig. 10. It shows that the correlation falls in the region of $\pm 20\%$ deviation and has a correlation coefficient of 0.989. It may be mentioned that rather than practical usage, this correlation is a framework on which future correlations over wider range of parameters can be built with greater amount of experimental data.

4. Conclusions

A set of convective heat transfer experiments with alumina-water nanofluids was carried out in the developing region of pipe flow with constant heat flux. The focal point of investigation was to evaluate the effect of particle size on convective heat transfer characteristics in the developing region. Two particle sizes were used, one with average particle size 45 nm and other with 150 nm. Following observations were made from the investigation.

- It was observed that both nanofluids, with 45 nm and 150 nm particles showed higher heat transfer characteristics than the base fluid.
- It was further observed that the nanofluid with 45 nm particles shows higher heat transfer coefficient than that with 150 nm particles. For instance at $x/D = 147$, for 45 nm particle based nanofluid (4 wt%) with $Re = 1550$, the enhancement in heat transfer coefficient was around 25% whereas for the 150 nm particle based nanofluids it was found to be around 11%.
- With increase in particle concentration and flow rate the average heat transfer coefficient value was increased.
- Also, it was observed that at the developing region the heat transfer coefficient is more than that at nearly developed region. For instance in 4 wt% nanofluid with average particle size 45 nm, at $Re \sim 1550$, the enhancement in heat transfer coefficient was 31% at $x/D = 63$, whereas it was 25% and 10% at $x/D = 147$ and 244, respectively. This may be due to

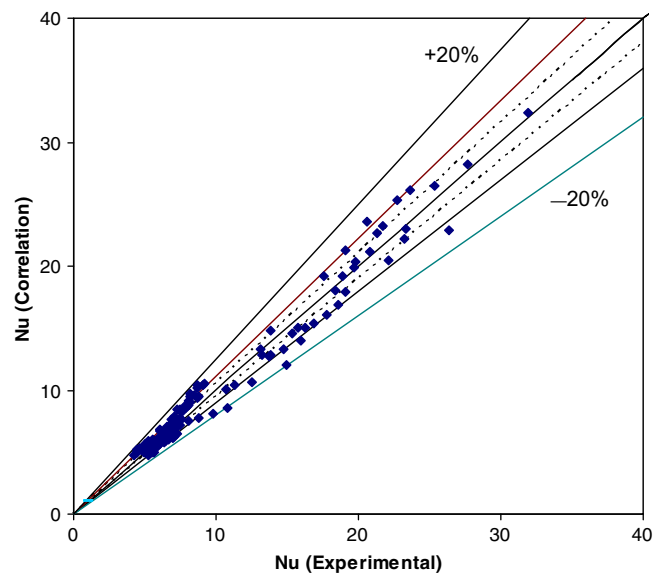


Fig. 10. Parity plot comparing the correlation and experimental results.

property variation in this region due to stronger temperature gradient along with the possibility of larger particle migration effect with lower particle sizes.

An experimental correlation was suggested to bring out effects of influencing parameters on convective heat transfer in the developing region while using nanofluids.

References

- [1] S.U.S. Choi, Enhancing thermal conductivity of fluids with nanoparticles, in: D.A. Singer, H.P. Wang (Eds.), *Developments and Applications of Non-Newtonian Flows*, vol. 231, ASME, New York, 1995, pp. 99–105.
- [2] S. Lee, S.U.S. Choi, S. Li, J.A. Eastman, Measuring thermal conductivity of fluids containing oxide nanoparticles, *J. Heat Transfer* 121 (1999) 280–289.
- [3] S.K. Das, N. Putra, P. Thiesen, W. Roetzel, Temperature dependence of thermal conductivity enhancement for nanofluids, *ASME J. Heat Transfer* 125 (2003) 567–574.
- [4] J.C. Maxwell, *A Treatise on Electricity and Magnetism* vol. 1, second ed., Clarendon Press, Oxford, UK, 1881.
- [5] R.L. Hamilton, O.K. Crosser, Thermal conductivity of heterogeneous two component systems, *Ind. Eng. Chem. Fundam.* 1 (3) (1962) 187–191.
- [6] B. Pak, Y.I. Cho, Hydrodynamic and heat transfer study of dispersed fluids with submicron metallic oxide particle, *Exp. Heat Transfer* 11 (1998) 151–170.
- [7] Y. Xuan, Q. Li, Investigation on convective heat transfer and flow features of nanofluids, *J. Heat Transfer* 125 (1) (2003) 151–155.
- [8] Y. Xuan, W. Roetzel, Conceptions for heat transfer correlation of nano-fluids, *Int. J. Heat Mass Transfer* 43 (2000) 3701–3707.
- [9] D. Wen, Y. Ding, Experimental investigation into convective heat transfer of nanofluids at the entrance region under laminar flow conditions, *Int. J. Heat Mass Transfer* 47 (2004) 5181–5188.
- [10] Y. Ding, D. Wen, Particle migration in a flow of nanoparticle suspensions, *Powder Technol.* 149 (2005) 84–92.
- [11] Y. Ding, H. Alias, D. Wen, A.R. Williams, Heat transfer of aqueous suspensions of carbon nanotubes (CNT nanofluids), *Int. J. Heat Mass Transfer* 49 (2006) 240–250.
- [12] Y.Z. Yang, G. Zhang, E.A. Grulke, W.B. Anderson, G. Wu, Heat transfer properties of nanoparticle-in-fluid dispersions (nanofluids) in laminar flow, *Int. J. Heat Mass Transfer* 48 (2005) 1107–1116.
- [13] C.T. Nguyen, G. Roy, C. Gauthier, N. Galanis, Heat transfer enhancement using Al_2O_3 -water nanofluid for an electronic liquid cooling system, *Appl. Therm. Eng.* 27 (2007) 1501–1506.
- [14] Y. He, Y. Jin, H. Chen, Y. Ding, D. Cang, H. Lu, Heat transfer and flow behaviour of aqueous suspensions of TiO_2 nanoparticles (nanofluids) flowing upward through a vertical pipe, *Int. J. Heat Mass Transfer* 50 (2007) 2272–2281.
- [15] S.Z. Heris, M.N. Esfahany, S.G. Etemad, Experimental investigation of convective heat transfer of Al_2O_3 /water nanofluid in circular tube, *Int. J. Heat Mass Transfer* 28 (2007) 203–210.
- [16] S.Z. Heris, S.G. Etemad, M.N. Esfahany, Experimental investigation of oxide nanofluids laminar flow convective heat transfer, *Int. Commun. Heat Mass Transfer* 33 (2006) 529–535.
- [17] G. Roy, C.T. Nguyen, P. Lajoie, Numerical investigation of laminar flow and heat transfer in a radial flow cooling system with the use of nanofluids, *Superlattices Microst.* 35 (2004) 497–511.
- [18] S.J. Palm, G. Roy, C.T. Nguyen, Heat transfer enhancement with the use of nanofluids in radial flow cooling systems considering temperature-dependent properties, *Appl. Therm. Eng.* 26 (2006) 2209–2218.
- [19] J. Buongiorno, Convective transport in nanofluids, *J. Heat Transfer* 128 (2006) 240.
- [20] W. Daungthongsuk, S. Wongwises, A critical review of convective heat transfer of nanofluids, *Renew. Sust. Energy Rev.* 11 (2007) 797–817.
- [21] H.E. Patel, S.K. Das, T. Sundararajan, N.A. Sreekumaran, B. George, T. Pradeep, Thermal conductivities of naked and monolayer protected metal nanoparticle based nanofluids: manifestation of anomalous enhancement and chemical effects, *Appl. Phys. Lett.* 83 (14) (2003) 2931–2933.
- [22] A. Bejan, A.D. Kraus, *Heat Transfer Handbook*, John Wiley and Sons, 2003.